THEORETICAL ANALYSIS OF EFFECTIVE CONDUCTIVITY OF METAL FOAMS WITH THERMAL INTERFACE MATERIAL

NUURUL SYAHIERAH BINTI OTHMAN

FACULTY OF ENGINEERING
UNIVERSITY OF MALAYA
KUALA LUMPUR

2018

THEORETICAL ANALYSIS OF EFFECTIVE CONDUCTIVITY OF METAL FOAMS WITH THERMAL INTERFACE MATERIAL

NUURUL SYAHIERAH BINTI OTHMAN

THESIS SUBMITTED IN FULFILMENT OF THE REQUIREMENTS FOR THE DEGREE OF MASTER OF MECHANICAL ENGINEERING

FACULTY OF ENGINEERING
UNIVERSITY OF MALAYA
KUALA LUMPUR

2018

THEORETICAL ANALYSIS OF EFFECTIVE CONDUCTIVITY OF METAL FOAMS WITH THERMAL INTERFACE MATERIAL

ABSTRACT

Effective thermal conductivity, k_{eff} of six (6) samples of two (2) configurations, between metal foams and thermal interface materials or called TIM, were measured at a maximum force of 45 N (Configuration 1) and 60 N (Configuration 2). The conductivity was measured in order to obtain its analytical value of each configurations or sample and then being compared with the theoretical value. The comparison and results of the test were further explained and discussed as well as the methodology. The TIM tester was developed in house based on ASTM D5470 standard test condition which used to determine the effective thermal conductivity, k_{eff} of thermally conductive solid electrical insulation materials. This tester was used to test all the six (6) samples. Most of the samples showed the trend of increasing conductivity over force applied. However, there is some uncertainty in the value mainly due to improper cooling or performance of the tester itself which discussed more in results and discussions part.

Keywords: thermal, effective thermal conductivity, metal foams, thermal interface material

THEORETICAL ANALYSIS OF EFFECTIVE CONDUCTIVITY OF METAL FOAMS WITH THERMAL INTERFACE MATERIAL

ABSTRAK

Termal efektif kekonduksian, k_{eff} untuk enam (6) sampel yang terdiri daripada dua (2) konfigurasi, yang mana terdiri daripada span logam dan bahan termal antara-muka atau dipanggil TIM, telah diukur pada tekanan tertentu dengan kadaran 45 N (Konfigurasi 1) dan 60 N (Konfigurasi 2). Kekonduksian itu diukur supaya nilai analitikalnya dapat diperolehi bagi setiap konfigurasi atau sampel seterusnya akan dibandingkan dengan nilai teori. Keputusan dan perbandingan setiap ujian dihuraikan dan dibincangkan bersama metodologinya. Alat penguji TIM telah direka bertepatan dengan piawai ujian ASTM D5470 yang digunakan untuk memperolehi termal efektif kekonduksian, k_{eff} bagi bahan penebat konduktif pepejal elektrik termal. Alat penguji ini digunakan bagi menguji keenam-enam sampel. Kebanyakan sampel menunjukkan trend kekonduksian menaik. Akan tetapi, terdapat juga beberapa ketidakstabilan nilai yang mungkin disebabkan oleh proses penyejukan yang tidak berfungsi dengan betul atau dari prestasi alat penguji itu sendiri yang akan dihurai dengan lebih lanjut di bahagian keputusan dan perbincangan.

Katakunci: termal, termal efektif kekonduksian, span logam, bahan termal antara-muka

ACKNOWLEDGEMENT

First of all, I am grateful to The Almighty God for establishing me to complete this research project together with this project report. I am also grateful to the God for the good health and wellbeing that were necessary to complete this research.

Foremost, I would like to express my sincere gratitude to my advisor Assoc. Prof. Dr. Poo Balan Ganesan for the continuous support and courage throughout my research. I am so much appreciating for his guidance and consistent support from the first day until this concluding moment. His guidance helped me in all time of research and writing of this report. I could not have imagined having a better advisor for my Master's Degree study. I also sincerely thanks for the time spent proofreading and correcting my mistakes.

Besides my advisor, my sincere thanks go to dearly Pn. Noor Fathiah binti Mohd Zaib which under the same research team, Thermal System Engineering Research team for being kind and helpful for me throughout my research and guiding me whenever I needed.

I acknowledge my sincere indebtedness and gratitude to my parents for their love, dream and sacrifice throughout my journey. I am also grateful to my husband who always stay by my side, sacrifice and motivate me. Special thanks should be given to my postgraduate friends for giving helps, comments and suggestions whenever I need. I cannot find the appropriate words to describe my appreciation to all of them for their devotion, support and faith in my ability to attain my goals.

TABLE OF CONTENTS

LIST OF FIGURES

LIST OF TABLES

LIST OF SYMBOLS AND ABBREVIATIONS

TIM: Thermal interface material

PCM: Phase change material

$\boldsymbol{k_{eff}}$: Effective thermal conductivity

LED: Light emitting diode

PPI: Pore per inch

PC94: Types of TIM (thermal conductive pad)

$\boldsymbol{cm^2}$: Centimeter cubic

$\boldsymbol{cm}$: Centimeter

$\boldsymbol{k}$: Conductance or conductivity

$\boldsymbol{W}$: Watt

$\boldsymbol{K}$: Kelvin

$\boldsymbol{Q}$: Heat transfer rate

$\boldsymbol{A}$: Surface area

$\Delta\boldsymbol{T}$: Temperature difference

$\boldsymbol{T_H}$: Temperature of hot region

$\boldsymbol{T_C}$: Temperature of cold region

d: Distance

ASTM: American Society for Test and Materials

$\boldsymbol{m}$: Meter

$\boldsymbol{s}$: Second

RTD: Resistance temperature detector

$\boldsymbol{L}$: Length

R: Thermal resistance

t: Thickness

N: Newton

LIST OF APPENDICES

CHAPTER 1

1.0 INTRODUCTION

1.1 Background

Metal foams are new generation of materials which were invented in the form of cellular structure. It consists of solid metal (for example aluminum, copper, etc.) with a composition of gas-filled pores whose contribute to most portion of the volume which likely to be known as porous metal as well. It can be classified as ultralight materials since the characteristics of this metal foams is high porosity materials (with only 5-25% base metal from its whole volume). These metal foams have gained interest among researcher to study their behavior and ability in flow regimes and also in hydrodynamics study Dukhan, Bağcı, and Özdemir (2014). Low densities, novel thermal, mechanical properties, electrical and acoustic properties of this new class materials offer great potential to be used in certain applications and fields.

Open-cell metal foams (**Figure 1.1**) will be used throughout the research as the percentage of porosity per unit volume is higher by having several kinds of thermal properties such as high conductivity, high permeability, lightweight, large area to volume ratio. Those properties made this type of metal foams suitable to be applied and used in various devices or applications including compact heat exchangers (Han et al., 2012), fuel cell(Yuan, Tang, Yang, & Wan, 2012), solar collectors(Chen, Gu, & Peng, 2010) and also in thermal storage units(Liu, Yao, & Wu, 2013).

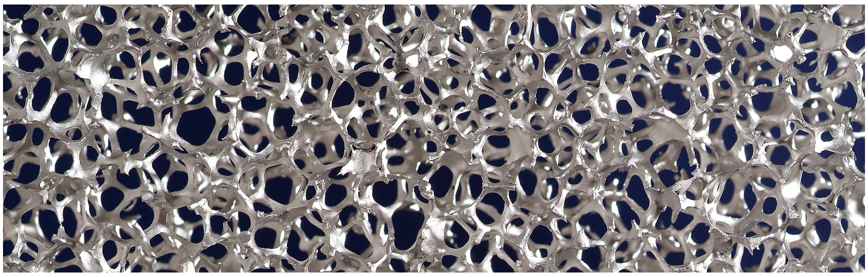

Figure1.1: Close-up image of open-cell metal foam, Source: https://www.ifam.fraunhofer.de/en/Profile/Locations/Dresden/Cellular_metallic_materials/offenzellige_metallschaeume.html

Further on this, novel systems associating metal foams and another combined material so-called thermal interface materials (TIM) open a broad range of new applications or as a new factor development (applications) in terms of high efficiency or thermally effective in recent years. TIM is a conductive material that been used as an interface material between surfaces or on a surface which functioned to replace the air trapped with the more thermally conductive material. It can increase the amount of heat transferred from the heat source into the heat sink significantly by creating a thermal path between the heat-generating component to the heat-sink (**Figure 1.2**).

However, the air is not fully removed because it is impossible to remove all air in most cases. The selection of TIM is crucial since it comes in many types and shapes (for example electrically isolating or electrically conductive, silicone base or silicone free, compliant or hard, solid or liquid or both, etc.) upon applications. The most popular TIM is gap fillers which made up from silicone in the form of elastomeric sheets used to increase the thermal conductivity of the material. The springy effects (due to its elastomeric base material) made it effective to be used in accommodating tolerance stack-ups and multiple devices.

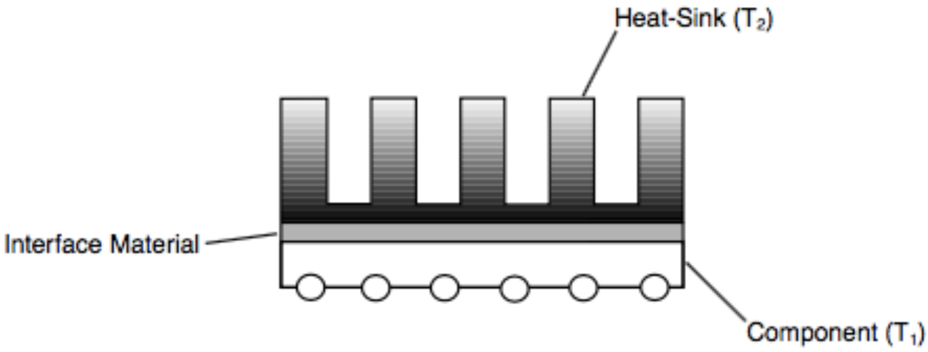

Figure 1.2: Thermal interface application (thermal path between heat generating component and a heat sink) Source: 3M Technical Bulletin, Characteristics of Thermal Interface Materials, (January,2001).

Therefore, the versatility and function ability of this materials (metal foams) have its own potential to be developed as a compact heat exchanger. However, it is not feasible in term of cost, manufacturing and process for large scale purpose as this material is still brand-new and fresh in this years. Other than that, the capability of this material still demand for more research and studies to be carried out to be proven as the most prominent material and can be the best replace over the present materials used. So, a study of thermal effective conductivity has been carried out. The study of thermal conductivity is important to analyze the performance and the ability of the configurations (combined materials or sandwiched materials with metal foams) that will be used in developing a heat exchanger.

1.2 Problem Statement

The problem arises when the surface (leg based) of the metal foam itself may not be uniform due to manufacturing process, the norm of the structure and maybe due to the cutting process; this create uneven contact between two contact surfaces (between metal foam and interface materials or other materials) and may cause impeding of the heat flow.

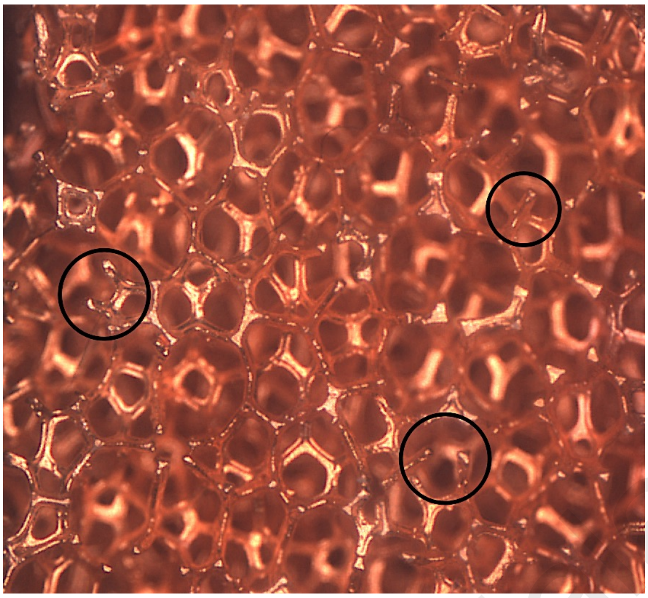

Figure 1.3: Uneven structures of copper foams causing thermal impedance

Therefore, the usage of TIM may serve as the best interface materials in the means of providing good connectivity of two (2) different materials or metals. However, the effective selection of different types of TIM with metal foam is still not known.

1.3 Objectives

This research project represents two (2) main objectives;

1. To carry out theoretical calculations of thermal effective conductivity of the combination of metal foams and TIMs into several configurations.

2. To evaluate the accuracy of the prediction with experimental results.

1.4 Scope and Limitation

The main scope of this project is performing the analytical evaluation of metal foams and TIMs by forming them into different configurations. With that, the prediction of the thermal effective conductivity, $\boldsymbol{k_{eff}}$ can be made to all of them (samples).

The determination of the k_{eff} involves many process and procedure. In order to obtain the k_{eff} of the sample, certain amount of force need to be applied to the sample. However, there is no maximum limit of force need to be applied to each of the sample. This is because excessive force may overly damage the sample and result to inaccuracy and instability.

1.5 Research Report Outline

- Chapter 1 outlines the overall project background, problem statement, objectives and scope of the study. A general overview of the research project is summarized.

- Chapter 2 reviews the research studies that have been done by the previous researchers in this related field for better understanding in thermal conductivity as well as metal foams. It is also covers the applications and approaches used in order to understand the concept and trends.

- Chapter 3 describes the clear explanation on the approaches used upon project completion. The justifications of the data collection and the methods are compiled.

- Chapter 4 details the results and discussion based on the experimental results from the data obtained and performing analytical calculations. The discussions are then being made based on the research study.

- Chapter 5 summarizes overall research findings in a conclusion. Thus, some recommendations also suggested for future improvement in this related field of study.

CHAPTER 2

2.0 LITERATURE REVIEW

2.1 Metal foams

Thermal conductivity is one of the important factor that being applied in many engineering applications or fields, especially in thermal management-related applications. Nowadays, the emerging of thermal conductive materials is at rise when researchers are trying to form many types of thermally conductive materials from other materials like plastics or by producing new materials such as metal foams and form them (metal foams) into several configurations with other materials. Metal foam is known of their outstanding mechanical and physical properties, flexibility (easy to achieve optimal stiffness and can withstand great damage with little deformation) and low weight (Liu & Chen, 2014). Because of that, it is best to be used in most of thermal applications.

Metal foams or cellular metals can be classified as open-cell or closed cell. Open-cell foam is referring to cells that interconnected between one another (no walls), so that fluid can easily pass through it. While closed-cell foam, the cells compose individual enclosure within the material. Compared to other materials (non-cellular materials), open-cell types have high heat transfer potential, high gas permeability as well as high thermal conductivity. For closed-cell types, it is more on thermally insulating characteristics. However, both of them have great properties of good impact energy absorption, resistance to thermal shock and have high strength and toughness which suitable for high pressure applications. The porous-type surface made their morphology easily to be controlled (during the production or manufacturing process) by adjusting their pore size and pore distribution per unit area (Liu & Liang, 2001; H. P. Tang, Liao, & Zhu, 2007; Tuchinskiy, 2005).

Open-cell metal foams are characterized by a high porosity, usually contain more 85% of porous area which considered as the most effective materials to improve the rate of heat transfer due to their high thermal conductivities and high surface area densities. Bhattacharya *et.al* (2002) have been carried out a comprehensive experiment in providing an analysis of estimating the effective thermal conductivity of high porosity metal foams. It shows that the effective thermal conductivity is strongly dependent to the porosity and also the ratio of the cross-sections (Bhattacharya, Calmidi, & Mahajan, 2002).

There are several studies that investigate thermal conductivity of high porosity metal foams like (Boomsma & Poulikakos, 2001) and (Zhao, Kim, Lu, & Hodson, 2004). Huisseune (2014) used metal foams as their design optimization of heat exchangers which revealed the uniqueness and advantages of open-cell metal foam itself. He also claims that improving current designs somehow is crucial and but by using new materials somehow much easier and better performance (Huisseune H.*, 2014). It seems that metal foam is the most prominent as compared to others. In most application, open cell metal foams being used as sandwich panels with other types of materials or with foam type materials as well like closed-cell metal foam. It is another merit to be considered as multifunctional structures (J. Tian, 2004).

Alike thermal conductivity, k_{eff} is much desire when dealing with samples or configuration that involve combination of one or more materials (whether they are from the same type of materials or might be different types). Previous years, there was an experiment that evaluated k_{eff} of open cell composite-alloy metal foams with different porosities and pore dimensions. The measurements of k_{eff} obtained is then compared with numerical predictions by using lattice-Boltzmann method in order to form new simplified numerical solutions from the foam geometry obtained (Wulf et al., 2014).

In the same year, Xiao et al (2014) doing a study regarding latent heat storage of open-cell metal foams and how thermal conductivities affect them. Metal foams (different porosity and PPI) are used to bombard the conductivity of phase change material, PCM, under a steady-state system. As the result, it shows good agreement with theoretical predictions and the usage of metal foams finally enhanced the conductivities of the PCMs about forty four times larger than of the pure (Xiao, Zhang, & Li, 2014). Next, a study on different porosities and pore sizes of aluminum sponge (open-cell foams) was carried out in order to study the k_{eff} by using the replication technique (produce samples of porosity between 0.57 to 0.77 and pore sizes between 0.7 mm and 2.4 mm) the perfect correlation was achieved at 0.5 to 1.0 porosities (Abuserwal, Elizondo Luna, Goodall, & Woolley, 2017).

2.2 Thermal Interface Materials (TIM)

TIM is design to transport out the accumulated heat from the heat source. It helps to avert thermal resistivity caused by the small gap (due to uneven contact surface). Losing heat will subject to a low thermal conductivity of the whole configurations. Improving thermal dissipation (losing heat) required good attainment of thermal contact otherwise the usage of thermally conducting materials is just a waste. That's why TIM is commercially important in most of thermal applications (Gopal, Whiting, Chew, & Mills, 2013; Jeng, Chen, & Cheng, 2006; Lishchuk et al., 2018).

TIM come in various forms and shapes, like thermal fluids, thermal greases (pastes), resilient thermal conductors, solders (in molten state) and phase change materials, PCM (change the solid state to liquid state). The thermal fluids, thermal greases, molten solder or molten PCM is spread on the mating surfaces upon usage. Then, for resilient thermal conductor normally it can be sandwiched with the mating surfaces and held in place by pressure. Thermal fluids commonly made up from mineral oil. Thermal greases (pastes) are commonly from conducting particle (usually metal or metal oxide) filled silicone.

However, upon usage of liquid or semi-liquid kind of TIM gives unfavorable conditions where it tends to flow out. So, another way to tackle it, is by using the TIM which in solid state at room temperature and might be in the liquid or semiliquid state at a slightly higher temperature. Another type of TIM is resilient thermal conductors which most commonly made up from conducting particle filled elastomers. Above all these TIMs, thermal greases and solder are mostly used and easy to find in terms of availability (Damian, Branescu, & Soare, 2012; Maguire, Behnia, & Morrison, 2005).

Furthermore, the query on their effectiveness might arise and this come along with thermal conductivity. The most effective TIM is said that the one which have high value of heat conductivity, which depends on the selection (types of TIM) and application of the TIM itself, and the material to be interfaced as well. It is proven that by using good thermal conductor materials as base material (or material to be interfaced), will result high thermal conductivity and thus enhancing the effectiveness of the TIM (Dmitriev & Valeev, 2017; Qiu et al., 2016).

TIM is one of the famous material due to high demand in most electrical and electronics which related to thermal concepts applications. The emergence of this material has brought an interest in combining or re-characterize them with nano materials and also any other materials like polymer and many more. There was a study on advancement of electrically conductive adhesives as new generation of TIM which seen to replace solder in electronic packaging industry (Li & Wong, 2006). Y.Tang (2016) studied and carried out a research on thermal performances of light-emitting diode (LED) using three different types of TIM . The result shown that by using graphene as interface material the temperature of the LED decrease sharply. The implication can be made was, graphene might be a potential for thermal design in LED and will creates future research directions especially for study of LED (Y. Tang, Liu, Yang, & Yang, 2016).

2.3 Summary of Previous Study and Research Gap

Although there were many researchers studying on the metal foams as well as thermal conductivity, none of them focusing on evaluating effective thermal conductivity of a configurations. In deep, which consists of layered materials of any type of metal foams with any types of TIM (as a configuration). Most of the studies are more on determining specific conductivity of a metal foam its own or any type of TIM its own. Some of them doing prediction and improvement also advancement on the method or the materials in order to improve its performance as well as its thermal conductivity.

Therefore, to fill up this gap, this research was conducted for determining the prediction of thermal effective conductivity of several configurations that consists of copper foams and TIMs. Copper foams with 20 PPI, 40 PPI and 60 PPI were layered with thermal pad (as TIM) to form into different configurations. The prediction of their effective thermal conductivity has been obtained after being tested using in-house TIM tester. Experiments were carried on for six (6) samples in total.

CHAPTER 3

3.0 METHODOLOGY

3.1 Preparation of Samples (Different Configurations of Metal Foams with TIMs)

Six (6) samples were prepared consist of different PPI of metal foams and TIMs, two (2) configurations as in **Figure 3.1** are formed by sandwiching the metal foam with TIM layered by layered. Upon completing the preparation stages, the samples prepared were kept in an airtight container in order to prevent deformation (as the materials are easy to deform) also to avoid reaction with surroundings before their conductivity being tested and analyzed. All the preparations and lab procedures were carried out at Thermal Laboratory, Level 4, Faculty of Engineering, University of Malaya. **Table 3.1** shows all the samples tested.

Figure 3.1: Configurations of sandwiched metal foams and TIMs bounded with copper plate
(left side: Configuration 1, right side: Configuration 2)

Table 3.1: Table of samples tested throughout the research study

Configurations	Samples	Plate	TIM	Copper foams
1 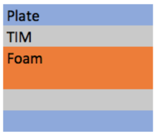	1			20 PPI
	2	Copper plate	TIM PC94	40 PPI
	3			60 PPI
2 	4			20 PPI
	5	Copper plate	TIM PC94	40 PPI
	6			60 PPI

3.1.1. Preparation of Metal Foams

The metal foams were purchased from local manufacturer of thermal appliances and the metal foams used were copper type due to its effectiveness and high efficiency in most thermal applications. In this project, different pore density (or PPI) of metal foams is used, which ranging from 20 to 60 PPI with same porosity of 98%. The metal foams are then being cut into smaller pieces with 1.8 cm square shape which seems to be the best fit and suitable measurement for the experiment to be further carried on. **Figure 3.2** below shows the sample of the metal foams used.

Figure 3.2: Metal foams of different pore density in 1.8 cm square shape

3.1.2. Preparation of TIMs

The TIM was purchased from the local manufacturer thermal appliances company. In order to conduct the project, non-silicone thermal conductive pad (PC94) type of TIM is chosen to be used throughout the project, refer **Figure 3.3**. The preparations are almost the same to that of metal foams but this time it took shorter time and much easier due to its soft kind material and rigid so, it is easy to cut into the selected area of 3.24 cm^2 square shape. Lastly, both metal foams and TIM are being sandwiched to form two (2) different configurations which each configuration made up of 3 different PPI of metal foams (20 PPI, 40 PPI and 60 PPI). Refer **Appendix A** for more details on features and properties of chosen TIM.

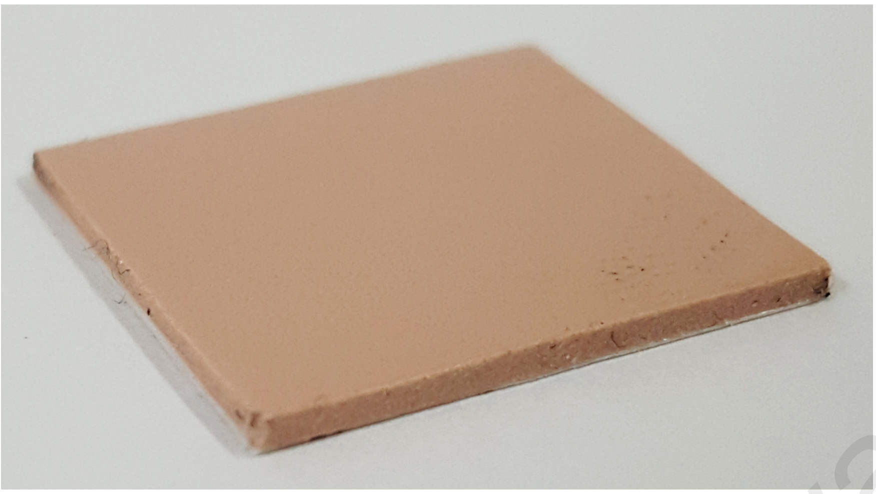

Figure 3.3: PC94 Thermal conductive pad in 1.8 cm square shape

3.2 Formulation and Method Analysis

A steady state method was used in order to determine the thermal effective conductivity, k_{eff} of the sample configurations (sandwiched of metal foams and TIM). This method is approximately close to the actual conditions in most TIM-related cases for example, heat flows through a sandwiched TIM between two surfaces under certain clamping pressure. Under these circumstances, there will be a linear gradient of the temperature throughout the system and the k_{eff} can be calculated using explicit heat transfer equations.

The conductance can be determined by finding the ratio of the heat flux to the temperature drop which govern in Fourier's law as in **Equation 1** below.

$$k = \frac{Q}{A(\Delta T)} = QA^{-1}\Delta T^{-1} \quad (1)$$

where k is the conductance of the sample in W/cm^2K, Q is the heat transfer rate across the sample, A is the surface area of the samples in cm^2, ΔT is the temperature difference from hot region, T_H to the cold region, T_C. The temperature is taken at different point along the meter bars so that the value T_H and T_C can be determined. Otherwise, it could not possible to find it directly. The interpolation of the temperature drop across the sample and the meter bar could be, **Equation 2**;

$$\left(\frac{dT}{dX}\right)_{hot} = \frac{\Delta T_{1-3}}{d_{1-3}}\ ,\ \left(\frac{dT}{dX}\right)_{cold} = \frac{\Delta T_{4-6}}{d_{4-6}} \tag{2}$$

Then, the heat flux through the meter bar and sample is then determined by using the temperature drop across the meter bars and the thermal conductivity of the meter bar material. The heat flux is calculated as the average of the heat flux measured in hot and cold meter bars, so it simply forms (**Equation 3**),

$$Q = kA\left[\frac{\frac{\Delta T_{1-3}}{d_{1-3}} + \frac{\Delta T_{4-6}}{d_{4-6}}}{2}\right] \tag{3}$$

The combination of all equations above, Equations 1, 2 and 3 could be useful to calculate the effective thermal conductivity of the sample as a function of the temperature measurements, meter bar and its thermal conductivity as follows (**Equation 4**);

$$k_{eff} = \frac{\left[\frac{k}{2}\left(\frac{\Delta T_{1-3}}{d_{1-3}} + \frac{\Delta T_{4-6}}{d_{4-6}}\right)\right]}{\left[\Delta T_{3-4} - d_{3-H}\frac{\Delta T_{1-3}}{d_{1-3}} - d_{C-4}\frac{\Delta T_{4-6}}{d_{4-6}}\right]} \tag{4}$$

3.3 Development of TIM Tester

The tester was modeled according to the ASTM D5470, see **Figure 3.4** standard test condition which used to measure the effective thermal conductivity of thermally conductive solid electrical insulation materials.

Custom press was built to apply certain clamping pressure to the sample. The vertical adjustment which consist of screw will help to apply the force by turning so that the pressure will transferred directly to the sample under pressing condition. The clamping pressure is measured manually using the dial gauge which positioned at the two surfaces of the middle sliding plates (acrylic plates). The clamping pressure is then calculated manually referring to the dial gauge reading recorded during running the test.

In order to approximate a one direction heat transfer, the hot part and the cold part of the metal bars were insulated using a thick layer of ceramic fiber wool insulation by wrapping around the metal bars (attached during running the test) to prevent from heat losses to the air. To avoid the acrylic surface to be melt (due to the heat generated by the cartridge heater), ceramic insulation is used and attached between the acrylic surfaces and the top surface of the metal bar which also known as heating part. The last part before the spring is the cooling part where the medium used is water. So, the water from the source will flow across the tester to the tank to provide the cooling effect during the testing run. The velocity of the water flow of 1.73 ms^{-1} is fix for all six samples tested.

Data were collected using MadgeTech 4 Data Loggers, Oct RTD from the installed MadgeTech Software. Upon installation and calibration, the system is automatically configuring the loggers by reading the device type by the host computer. This system is channel based, six (6) channels were used which refer to six (6) point of RTD or temperature points (as in **Figure 3.4** the RTD points are from T1 to T6). The example summary of the average data series obtained from the data loggers as well as description of Oct RTD used were attached in appendix section, **Appendix B** and **C**.

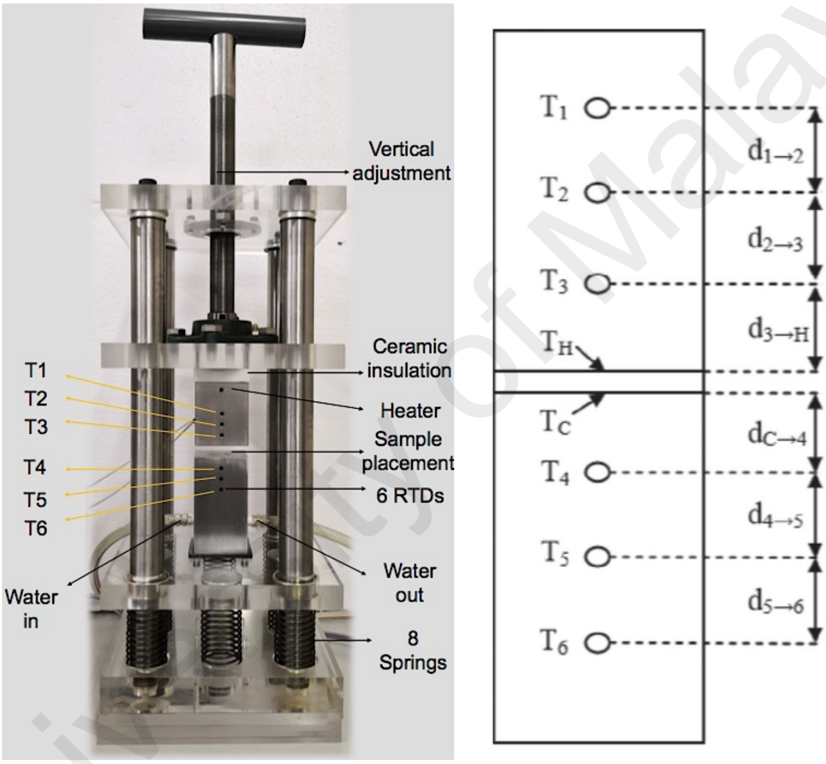

Figure 3.4: Labelled photograph and labelled schematic diagram of the TIM tester

3.4 Testing of Effective Thermal Conductivity Using In-House TIM Tester

In this work, six (6) different samples are tested (refer **Table 3.1**) using in-house tester in order to obtained their effective thermal conductivity, k_{eff} . The first step before testing took part, is the setup preparation of the tester itself. The test surfaces of the metal bar need to be cleaned so that there is no unwanted residue stick on the samples or on the metal bars surfaces. All the samples are solid and being tested under normal room condition.

In order to ensure the movement of the sliding plates smooth, some amount of grease was spread over the surface of the aluminum bar and also at the screw so it is smooth and easy to be turned. Once the sample is placed in its position, the screw will be turned until there is no gap between the sample surface and the metal bar surface. The heater must be switched on, as the water flow and the system must be ready before it is allowed to reach the steady state. The cartridge heater was set to 80 °C. Before run, it is important to ensure that the area around the metal bar (hot and cold region) be covered with ceramic fiber wool to prevent the heat from escape to the environment.

Once the system run about a minute, steady state reached, pressure was applied via screw turning for 10 seconds and rest 10 seconds (alternately and repetition) until the sample damage due to the pressure applied. While turning, the dial gauge reading was recorded and the clamping force can be calculated for further analysis. Temperature data from the six (6) RTDs was set to be recorded at every 5 seconds. The test stop once it reaches the maximum limit (sample damage) and the software will be ended in order to get the series of temperature data.

Calculations and data analyzing were done using manual calculations and analyzed using Microsoft Excel Spreadsheet. Referring to the data series obtained, the average temperature of six (6) RTDs were then calculated. These temperature differences were used to calculate the k_{eff} of the samples at difference clamping pressure.

CHAPTER 4

4.0. RESULTS AND DISCUSSIONS

4.1. Analytical Calculations and Comparison

The analytical calculations begin with determination of theoretical so that it can be compared to the experimental once the test completed. The theoretical was developed by using the concept of thermal resistance where the temperature distribution is in a straight line under the steady heat conditions. The k_{eff} could be obtained from the ratio of the total length, L_{total} to the total resistance, R_{total} of the whole configuration since the study is under the heat conduction case.

Table below shows the parameters of the materials used,

Table 4.1: Table of conductivity and thickness of the materials used in this study

Materials	Conductivity, k (W/mK)	Thickness, t (m)
Copper plate	270	0.0005
TIM PC94	4	0.001
Copper foam	3	0.005

The conductivity of the copper plate and the TIM PC94 were obtained from the products specifications from the manufacturer while the conductivity of the copper foam was obtained from the previous study of the research team. These parameters used for both configurations (refer **Figure 3.1**) as the materials used were also same. Now, the thermal resistance for each material could be obtained as in **Table 4.2** and **Table 4.3** follow,

Table 4.2: Thermal resistance, R of all materials for Configuration 1

Materials	Thermal resistance, $R\ (m^2K/W)$
Copper plate	$3.7037E^{-6}$
TIM PC94	$0.5E^{-3}$
Copper foam	$1.667E^{-3}$

Table 4.3: Thermal resistance, R of all materials for Configuration 2

Materials	Thermal resistance, $R\ (m^2K/W)$
Copper plate	$3.70376E^{-6}$
TIM PC94	$0.75E^{-3}$
Copper foam	$3.333E^{-3}$

The R was calculated for two (2) copper plates, two (2) TIMs and a copper foam for the first configuration and two (2) copper plates, three (3) TIMs and two (2) copper foams for the second configuration (refer **Figure 3.1**).

Effective thermal conductivity, k_{eff} can be calculated by using the total thermal resistance, R_{total} and the total thickness as L_{total} for both configurations. Thus, it can be used as the theoretical predictions for this study. **Table 4.4** tabulated all the values to determine the k_{eff}.

Table 4.4: Theoretical determination of k_{eff} for both configurations

Configurations	Total thickness, L_{total} (m)	Total thermal resistance, R_{total} (m^2K/W)	Effective thermal conductivity, K_{eff} (W/mK)
Configuration 1	0.008	0.0021704	3.686
Configuration 2	0.014	0.0041288	3.425

Based on the k_{eff} obtained, it was aimed to have higher k_{eff} for the second configuration since it involves with more materials like foams and TIMs in order to dissipate heat. However, Table 4.4 shows that the k_{eff} for the first configuration slightly higher to the second configuration by 7%. This is because, higher resistance of the configuration will be resulted lower k_{eff} since resistance is inversely proportional to k_{eff} but directly proportional to L_{total}.

This means, by having more thickness, the resistance will become higher as the heat travel for certain distance of the configuration and there might be some amount of heat escaping to the air before it reaches to the end point and thus, the k_{eff} of the configuration will become lower. There is no way to avoid it from happening since it happens naturally because the material itself conductive. From here, it can be concluded that, Configuration 1 have the better k_{eff} theoretically.

4.2. Experimental Results from In-House Tester and Comparison

After undergoes all the methodology, the data series being analyzed so that further calculations could be carried on in order to get the experimental results of the study. First and foremost, the temperature difference from the data series of all samples were tabulated according to addition of every 5N force applied. It is important to ensure that the temperature data were taken at the specific local temperature. The data series are actually the RTD readings recorded by the data loggers during the test run. In order to get k_{eff} of each sample (which consists of 20 PPI, 40 PPI and 60 PPI metal foams with TIMs of different configuration), all the values and parameters are substituted into the **Equation 4** as in Chapter 3.

However, there are certain values are fix (conductivity of metal bar, distance between two RTDs, and distance from RTD to samples) for all samples as in **Table 4.5** below, for the other parameters, the values were obtained from the temperature differences at each local point (at every 5 N force applied).

Table 4.5: Fix values of certain parameters

k, W/mK	d_{1-3}, m	d_{4-6}, m	d_{3-H}, m	d_{C-4}, m
205	0.008	0.008	0.008	0.008

The force applied for all samples (both configurations) are as in **Table 4.6**, they were figured out manually using Hooke's Law, spring constant from the dial gauge reading data recorded at each sample's test. The average of every 5 N of the force applied will helps to locate their temperature distribution at each local point, which seems practical to be used in determination of k_{eff} of each sample.

Table 4.6: Table of applied force for both Configuration 1 and Configuration 2

<table>
<tr><th>Configurations</th><th>Samples</th><th>Force Applied, F (N)</th></tr>
<tr><td rowspan="3">1
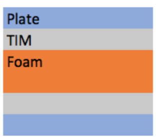</td><td>1</td><td>73.083</td></tr>
<tr><td>2</td><td>78.542</td></tr>
<tr><td>3</td><td>81.462</td></tr>
<tr><td rowspan="3">2
</td><td>4</td><td>77.127</td></tr>
<tr><td>5</td><td>76.294</td></tr>
<tr><td>6</td><td>76.791</td></tr>
</table>

The summarized of k_{eff} values of all samples with addition of 5 N applied force for Configuration 1 (refer **Table 3.1**) are tabulated below (**Table 4.7, 4.8 and 4.9**), the whole complete calculation spreadsheets are attached to the appendix in the last section of this report.

Table 4.7: Data results of k_{eff} for Configuration 1 with 20 PPI copper foams

Addition of force every 5 N (N)	Effective thermal conductivity, k_{eff}, (W/mK)
5	0.9881
10	0.9589
15	1.2350
20	1.3712
25	1.5647
30	1.6463
35	1.6025
40	1.6800
45	1.7964
50	1.7929
55	1.6899
60	2.1789
65	2.1903
70	2.3349

Table 4.8: Data results of k_{eff} for Configuration 1 with 40 PPI copper foams

Addition of force every 5 N (N)	Effective thermal conductivity, k_{eff}, (W/mK)
5	1.0051
10	1.3585
15	1.5579
20	1.6719
25	1.7259
30	1.8320
35	1.9140
40	1.9913
45	2.0788
50	2.0388

55	2.0638
60	1.9830
65	1.9538
70	1.9876
75	2.0045

Table 4.9: Data results of k_{eff} for Configuration 1 with 60 PPI copper foams

Addition of force every 5 N, F (N)	Effective thermal conductivity, k_{eff}, (W/mK)
5	1.2177
10	1.5296
15	1.6697
20	1.8236
25	1.9535
30	2.0368
35	2.1174
40	2.1936
45	2.2062
50	2.2388
55	2.2090
60	2.3329
65	2.2635
70	2.3426
75	2.3281
80	2.2366

The summarized of k_{eff} values of all samples with addition of 5 N applied force for Configuration 2 (refer **Table 3.1**) are tabulated below (**Table 4.10, 4.11 and 4.12**), the whole complete calculation spreadsheets are attached to the appendix in the last section of this report.

Table 4.10: Data results of k_{eff} for Configuration 2 with 20 PPI copper foams

Addition of force every 5 N, (N)	Effective thermal conductivity, k_{eff}, (W/mK)
5	1.2071
10	1.5612
15	1.8591
20	1.9997
25	2.0260
30	1.9457
35	1.9685
40	2.0191
45	1.9704
50	1.9875
55	2.0327
60	2.1039
65	2.0795
70	2.1917
75	2.0993

Table 4.11: Data results of k_{eff} for Configuration 2 with 40 PPI copper foams

Addition of force every 5 N, (N)	Effective thermal conductivity, k_{eff}, (W/mK)
5	1.3516
10	1.5933
15	1.8487
20	1.8544
25	1.9990
30	2.0074
35	2.1469
40	2.2190
45	2.4563
50	2.3961
55	2.4290
60	2.5880
65	2.5547
70	2.5843
75	2.4577

Table 4.12: Data results of k_{eff} for Configuration 2 with 60 PPI copper foams

Addition of force every 5 N, (N)	Effective thermal conductivity, k_{eff}, (W/mK)
5	2.0235
10	2.2681
15	2.6238
20	2.7665
25	2.9500
30	2.9242
35	3.1767
40	3.1476
45	3.1983
50	3.2486
55	3.3778
60	3.3877
65	3.4294
70	3.4330
75	3.5859

The data for all samples of Configuration 1 and Configuration 2 could be presented as in **Figure 4.1** and **4.2**. Both graphs show the behavior of the k_{eff} with the addition of force applied at every 5 N for all three (3) samples of Configuration 1 and 2. It is seen that an increase of force leads to considerable increase in k_{eff} which resulted a positive trend of all samples. However, there are uncertainties along the trend for both configurations. This uncertainty might due to the small temperature drop across the heat flux. Therefore, by increasing the heat flux could be the best solution so that the temperature drop could be increased as well. But, there is limitation to apply higher amount of heat flux by the cooling rate through heat sink, otherwise the cooling rate need to be match to that of increasing amount.

There was instability to the samples with 20 PPI copper foams for both configurations that could be observed throughout the test. It is mainly due to its morphological structure which caused uneven surfaces as compared to 40 and 60 PPI copper foams (refer **Figure 3.2**). Small number of pore per inch but large size of pores resulted low $\mathrm{k_{eff}}$ of 20 PPI copper foams since the volume of the copper contains in the materials is also small which affected the whole configuration of the sample. In other words, thermal dissipation has occurred throughout the test (due to the gap between contacted surfaces), it can be improved but required good attainment of thermal contact between the conducting materials.

Samples with 40 and 60 PPI copper foams for both configurations show their stability towards increasing k_{eff} although there are some fluctuations at certain force applied. The fluctuations might be due to off-balance during turning process since it be done manually. It also happens to the samples with 20 PPI copper foams for both configurations.

There were obvious gaps between each of the sample trends in **Figure 4.2** of Configuration 2 might due to the repeated usage of the equipment causing the deformation at the surface of the meter bars which possible to be happened. Over numbers of test runs, this somehow modified the surface roughness of the meter bars. Other than that, there might have contamination at the meter bars surface which not being removed by the proper cleaning procedure. To test with new meter bars every test run seems impossible but this matter should be taken seriously to avoid inaccuracy.

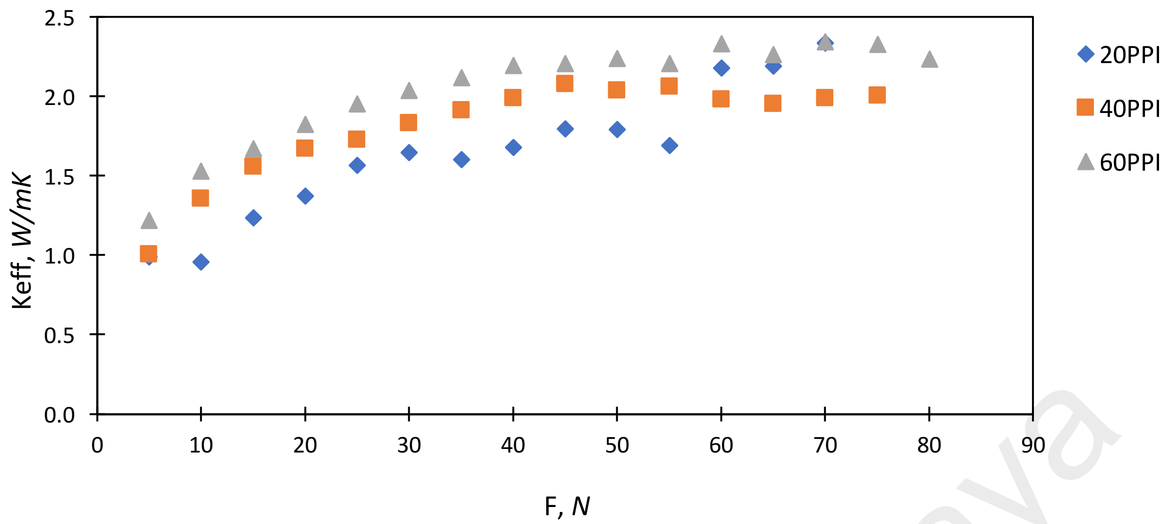

Figure 4.1: Graph of k_{eff} against force for Configuration 1

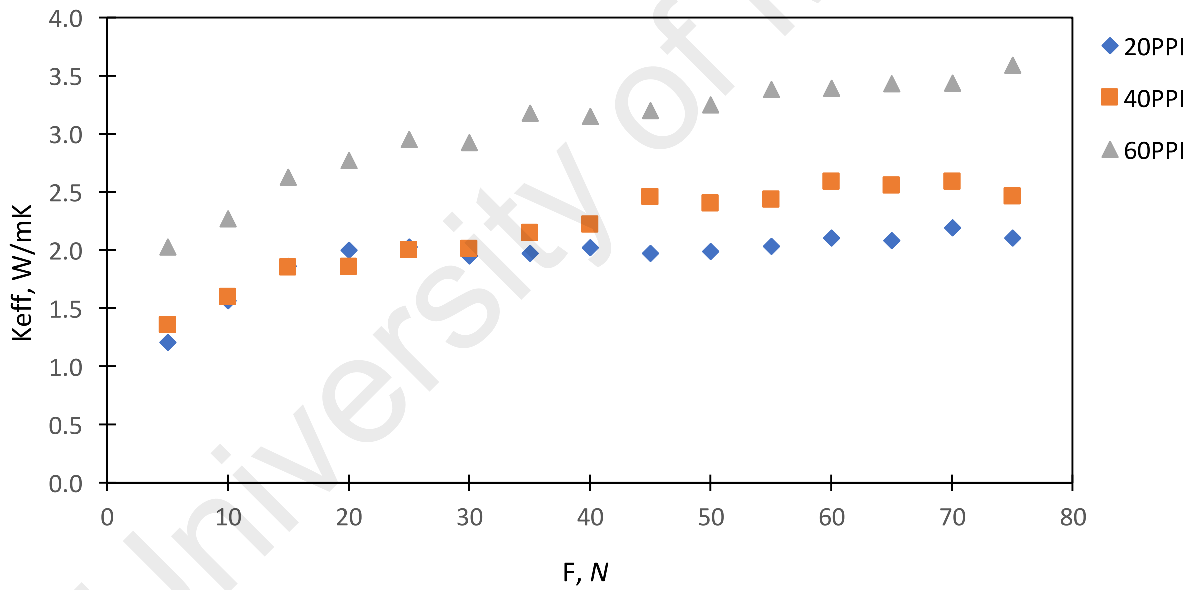

Figure 4.2: Graph of k_{eff} against force for Configuration 2

Further to what has been shared earlier, following is the comparison between the theoretical and the experimental results. The value of k_{eff} at the maximum force applied is taken at 45 N for Configuration 1 and 60 N for Configuration 2. It is seen that instability to the conductivity-force trend when the force applied greater than 45 N (for Configuration 1) and 60

N (for Configuration 2). The tabulation has been made as in **Table 4.13**. The value of the k_{eff} of all samples (at maximum force of 70 N) then will be compared to those obtained by theoretical (refer subsection 4.1), percentage error also calculated and justifications been made as follows.

Table 4.13: Tabulation of comparison values of k_{eff} with percentage error of all samples

Configurations	Samples	Theoretical values of k_{eff}, (W/mK)	Experimental values of k_{eff} at maximum force of 45 N and 60 N, (W/mK)	Percentage error (%)
1 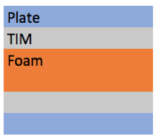	1	3.686	1.7964	51.3
	2		2.0788	43.6
	3		2.2062	40.1
2 	4	3.425	2.1039	38.6
	5		2.5880	24.4
	6		3.3877	1.1

*Note – Percentage error > 50% indicated thermal instability

From the table above, based on Configuration 1, sample 1 shows instability in thermal conductivity which may due to deformation occurred during the clamping by the large amount of force applied. Other than that, the materials condition is much more important. Any damages or deformity of foams or small defect of TIM will result to poor performance and low conductivity.

While for Configuration 2, sample 6 delivered very significant result at 1.1% of percentage error. This is due to the stability during the turning process so that the accuracy was maintained throughout the test runs.

Overall, beside sample 1 and 6, the rest delivered satisfactory results which indicates the uniformity of heat distribution along the test runs. It can be observed that k_{eff} of experimental results for Configuration 2 is much higher compared to Configuration 1, but theoretically supposed k_{eff} of Configuration 1 must be higher from Configuration 2. It might be due to different types or composition of copper foams used. This is because the conductivity of copper foams used in analytical calculations is taken from previous study. However, the k_{eff} of both study are comparable since the porosity of the copper foams used in both experimental and theoretical study is 98% porosity.

There is another factor that leads to inaccuracy of whole systems which is cooling system. Having more effective cooling system by maintaining the cooling capacity to the experimental heaters with low average temperature would result higher conductivity of the samples, but it requires some modifications to the tester.

CHAPTER 5

5.0 CONCLUSIONS AND RECOMMENDATIONS

In conclusion, the study involves six samples to be tested using the TIM tester under a steady state method. The samples consist of two different configurations showed an increasing trend of effective thermal conductivity, k_{eff} over an increase force applied or clamping force. The samples of Configuration 2 met the satisfactory which aimed to be the selected sample achieved, when all the samples are within the thermal stability resulted to lower percentage error compared to Configuration 1.

The work presented in this study is the first step towards achieving the performance of the copper foams-TIMs samples of their k_{eff} behavior analytically. It is necessary to address few points when dealing with foams-TIMs samples (or configurations). Firstly, it is important to make sure the correct and suitable TIM been chosen for the sample so that the thermal contact is good in order to avoid gap between the contacting materials and prevent heat dissipation.

The maximum clamping force or the force applied for each sample must be studied by testing it many times in order to get the optimum maximum force with the stability of the thermal distribution. So that, a better steady state condition could be resulted an optimum value of k_{eff} could be obtained. Over the full range of force applied to both sample studied, it shows that each sample have its own limits in order to maintain the stable heat distribution. Although the purpose of the force being applied is to make the sample damage, but higher force applied to the sample may give inaccurate results and the performance of the whole sample include

TIM will drop thus, the optimum value of k_{eff} could not be reached. This is also the reason why the maximum force applied were taken at 45 N for Configuration 1 and 60 N for Configuration 2 in this study.

Through this study, it can be concluded that k_{eff} is directly proportional to the force applied. As for this study, the samples of Configuration 2 delivered the better performance and achieved better stability in thermal conductivity distribution. Through the analytical calculations, the comparison being made to that of experimental result, the objective of this study has been achieved. This study can be reference to the future study of copper foams and TIMs but need to undergoes further study in order to fix the current limitations and capabilities.

REFERENCES

Abuserwal, A. F., Elizondo Luna, E. M., Goodall, R., & Woolley, R. (2017). The effective thermal conductivity of open cell replicated aluminium metal sponges. *International Journal of Heat and Mass Transfer, 108*, 1439-1448. doi:https://doi.org/10.1016/j.ijheatmasstransfer.2017.01.023

Bağcı, Ö., & Dukhan, N. (2016). Experimental hydrodynamics of high-porosity metal foam: Effect of pore density. *International Journal of Heat and Mass Transfer, 103*, 879-885. doi:https://doi.org/10.1016/j.ijheatmasstransfer.2016.07.097

Bhattacharya, A., Calmidi, V. V., & Mahajan, R. L. (2002). Thermophysical properties of high porosity metal foams. *International Journal of Heat and Mass Transfer, 45*(5), 1017-1031. doi:https://doi.org/10.1016/S0017-9310(01)00220-4

Boomsma, K., & Poulikakos, D. (2001). On the effective thermal conductivity of a three-dimensionally structured fluid-saturated metal foam. *International Journal of Heat and Mass Transfer, 44*(4), 827-836. doi:https://doi.org/10.1016/S0017-9310(00)00123-X

Chen, Z., Gu, M., & Peng, D. (2010). Heat transfer performance analysis of a solar flat-plate collector with an integrated metal foam porous structure filled with paraffin. *Applied Thermal Engineering, 30*(14), 1967-1973. doi:https://doi.org/10.1016/j.applthermaleng.2010.04.031

Damian, I., Branescu, C., & Soare, V. (2012, 25-28 Oct. 2012). *Solder paste optimization in thermal pad padstack.* Paper presented at the 2012 IEEE 18th International Symposium for Design and Technology in Electronic Packaging (SIITME).

Dmitriev, A. S., & Valeev, A. R. (2017). Graphene nanocomposites as thermal interface materials for cooling energy devices. *Journal of Physics: Conference Series, 891*(1), 012359.

Dukhan, N., Bağcı, Ö., & Özdemir, M. (2014). Metal foam hydrodynamics: Flow regimes from pre-Darcy to turbulent. *International Journal of Heat and Mass Transfer, 77*, 114-123. doi:https://doi.org/10.1016/j.ijheatmasstransfer.2014.05.017

Gopal, V., Whiting, M. J., Chew, J. W., & Mills, S. (2013). Thermal contact conductance and its dependence on load cycling. *International Journal of Heat and Mass Transfer, 66*, 444-450. doi:https://doi.org/10.1016/j.ijheatmasstransfer.2013.06.061

Han, X.-H., Wang, Q., Park, Y.-G., T'Joen, C., Sommers, A., & Jacobi, A. (2012). A Review of Metal Foam and Metal Matrix Composites for Heat Exchangers and Heat Sinks. *Heat Transfer Engineering, 33*(12), 991-1009. doi:10.1080/01457632.2012.659613

Huisseune H.*, D. S. S., Ameel B. and De Paepe M. (2014). Influence of Porosity and Pore Density on the Thermal and Hydraulic Performance of Metal Foam Heat Exchangers. *10th International Conference on Heat Transfer, Fluid Mechanics and Thermodynamics*.

J. Tian, T. K., T.J. Lu ,*, H.P. Hodson , D.T. Queheillalt, D.J. Sypeck, H.N.G. Wadley. (2004). The effects of topology upon fluid-flow and heat-transfer within cellular copper structures. *International Journal of Heat and Mass Transfer, vol. 47*, pp. 3171-3186.

Jeng, Y.-R., Chen, J.-T., & Cheng, C.-Y. (2006). Thermal contact conductance of coated surfaces. *Wear, 260*(1), 159-167. doi:https://doi.org/10.1016/j.wear.2004.12.041

Li, Y., & Wong, C. P. (2006). Recent advances of conductive adhesives as a lead-free alternative in electronic packaging: Materials, processing, reliability and applications. *Materials Science and Engineering: R: Reports, 51*(1), 1-35. doi:https://doi.org/10.1016/j.mser.2006.01.001

Lishchuk, P., Dekret, A., Pastushenko, A., Kuzmich, A., Burbelo, R., Belarouci, A., . . . Isaiev, M. (2018). Interfacial thermal resistance between porous layers: Impact on thermal conductivity of a multilayered porous structure. *International Journal of Thermal Sciences, 134*, 317-320. doi:https://doi.org/10.1016/j.ijthermalsci.2018.08.015

Liu, P. S., & Chen, G. F. (2014). Chapter Three - Application of Porous Metals. In P. S. Liu & G. F. Chen (Eds.), *Porous Materials* (pp. 113-188). Boston: Butterworth-Heinemann.

Liu, P. S., & Liang, K. M. (2001). Review Functional materials of porous metals made by P/M, electroplating and some other techniques. *Journal of Materials Science, 36*(21), 5059-5072. doi:10.1023/A:1012483920628

Liu, Z., Yao, Y., & Wu, H. (2013). Numerical modeling for solid–liquid phase change phenomena in porous media: Shell-and-tube type latent heat thermal energy storage. *Applied Energy, 112*, 1222-1232. doi:https://doi.org/10.1016/j.apenergy.2013.02.022

Maguire, L., Behnia, M., & Morrison, G. (2005). Systematic evaluation of thermal interface materials—a case study in high power amplifier design. *Microelectronics Reliability, 45*(3), 711-725. doi:https://doi.org/10.1016/j.microrel.2004.10.030

Qiu, L., Wang, X., Su, G., Tang, D., Zheng, X., Zhu, J., . . . Zhu, Y. (2016). Remarkably enhanced thermal transport based on a flexible horizontally-aligned carbon nanotube array film. *Scientific Reports, 6*, 21014. doi:10.1038/srep21014

Tang, H. P., Liao, J. C., & Zhu, J. L. (2007). Porous Metals of Northwest Institute for Non-Ferrous Metal Research. *Materials Science Forum, 534-536*, 1281-1284. doi:10.4028/www.scientific.net/MSF.534-536.1281

Tang, Y., Liu, D., Yang, H., & Yang, P. (2016). Thermal Effects on LED Lamp With Different Thermal Interface Materials. *IEEE Transactions on Electron Devices, 63*(12), 4819-4824. doi:10.1109/TED.2016.2615882

Tuchinskiy, L. (2005). Novel Fabrication Technology for Metal Foam. *Journal of Advanced Materials, vol. 37*, pp. 60–65.

Wulf, R., Mendes, M. A. A., Skibina, V., Al-Zoubi, A., Trimis, D., Ray, S., & Gross, U. (2014). Experimental and numerical determination of effective thermal conductivity of open cell FeCrAl-alloy metal foams. *International Journal of Thermal Sciences, 86*, 95-103. doi:https://doi.org/10.1016/j.ijthermalsci.2014.06.030

Xiao, X., Zhang, P., & Li, M. (2014). Effective thermal conductivity of open-cell metal foams impregnated with pure paraffin for latent heat storage. *International Journal of Thermal Sciences, 81*, 94-105. doi:https://doi.org/10.1016/j.ijthermalsci.2014.03.006

Yuan, W., Tang, Y., Yang, X., & Wan, Z. (2012). Porous metal materials for polymer electrolyte membrane fuel cells – A review. *Applied Energy, 94*, 309-329. doi:https://doi.org/10.1016/j.apenergy.2012.01.073

Zhao, C. Y., Kim, T., Lu, T. J., & Hodson, H. P. (2004). Thermal Transport in High Porosity Cellular Metal Foams. *Journal of Thermophysics and Heat Transfer, 18*(3), 309-317. doi:10.2514/1.11780